DETERMINISTIC *diagnostics*

Sudhendu Kashikar, Carl Neuhaus and Jon McKenna, MicroSeismic Inc., show how deterministic fracture diagnostics enhances the value of hydraulic fracture monitoring in unconventional resources.

Microseismic monitoring is the best technology for providing measurement of fracture propagation away from a borehole undergoing stimulation. The process of hydraulic fracturing generates stress in rocks, which is released in the form of fracturing, failure, and movement often along pre-existing natural fracture networks. This stress release generates microseismic waves that propagate outward from the source. These microseismic waves are detected by an array of surface, near-surface, or downhole geophones. The recorded signals are processed to determine the subsurface location of the fracture. As such, microseismic is principally a geophysical measurement. A lot of focus, research and engineering are being applied to improve the geophysical understanding and accuracy of the measurement.

One of the reasons for microseismic monitoring is to gain a better understanding of the efficiency and effectiveness of the hydraulic fracture geometry. To fully optimise the completion and hydraulic fracture treatment it is important to evaluate various aspects of the treatment's impact on the surrounding rock, such as differentiating propped and un-propped fractures, fracture growth and geometry, fracture overlap between stages and wells, stress shadowing effects and treatment efficiency. Today most of the fracture diagnostics are performed using various modelling techniques such as: geomechanical modelling, stochastic fracture modelling, reservoir simulation and history matching. These tools use microseismic pointsets to qualitatively calibrate the model – trying to gain an understanding of the underlying fracture properties. New methods are applied that combine contextual information such as geology, well logs, treatment data, etc. with deterministic analysis of the microseismic measurements to gain a deeper level of understanding.

This article will demonstrate new developments that enable valuable information to be extracted via the combination of contextual information with deterministic analysis of the microseismic pointsets. The methods discussed have been successfully implemented in multiple countries globally; however, this article will use examples from US basins. This distinct process of completions evaluation consists of a workflow and tools to perform diagnostic analysis of microseismic pointsets, enabling accurate evaluation of the fracture treatment. It is designed to deterministically characterise fracture network growth and complexity, while providing a methodology to evaluate the wellbore spacing, stage lengths, cluster spacing and treatment parameters.

Marcellus case study

A dataset collected from the acquisition array in Figure 1 was recorded in the near-surface with a permanently-installed array of 101 stations covering

an area of over 18 square miles that included five treatment wellpads. The Marcellus shale stretches over several states in the northeastern United States including New York, Pennsylvania, West Virginia and Ohio. As with all shale reservoirs, due to low matrix permeability, hydrocarbon production is dominated by the natural fracture networks present in the rock. In the Marcellus, the well-studied, pre-existing natural fracture sets are known as the J1 and J2.

After acquisition and data processing to determine the microseismic pointsets, a magnitude calibrated discrete fracture network (M-DFN) is modelled onto the microseismic events in two steps. The basic assumption is that every event is representative of a fracture, which can then be modelled and is centred on the event. Through source mechanism analysis, the strike and dip of the failure plane is identified for each individual event in step one. The characteristics of each individual failure plane are then determined through the microseismic magnitude of an event incorporating rock and fluid properties resulting in the M-DFN shown in Figure 2 in the second image. The microseismic event pattern and the orientations of the stimulated fractures show reactivation of the two sets of natural fractures – J1 and J2. The growth away from the wellbore follows the J1 fractures, in a northeast to southwest orientation,

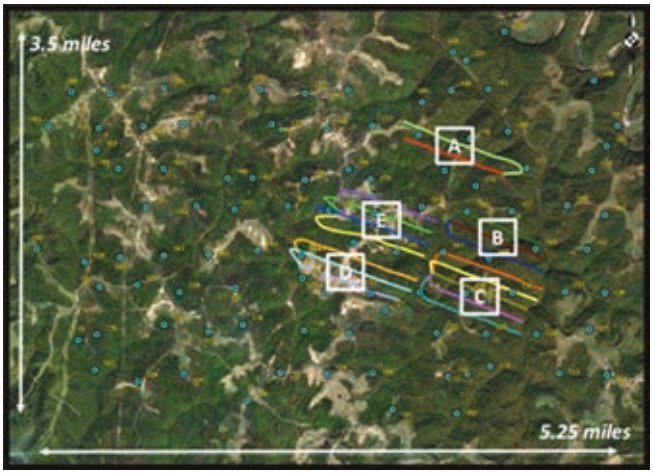

Figure 1. *Microseismic monitoring array. Recording stations can be seen as turquoise circles. Wellpads are named with letters.*

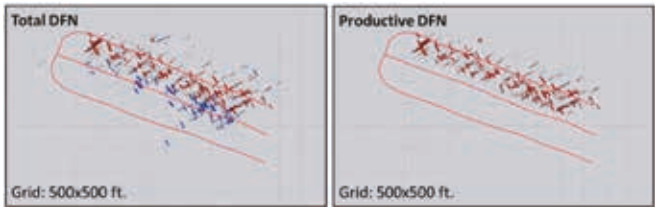

Figure 2. *The total DFN can be seen on the left. The proppant filled portion of the total DFN can be seen in red.*

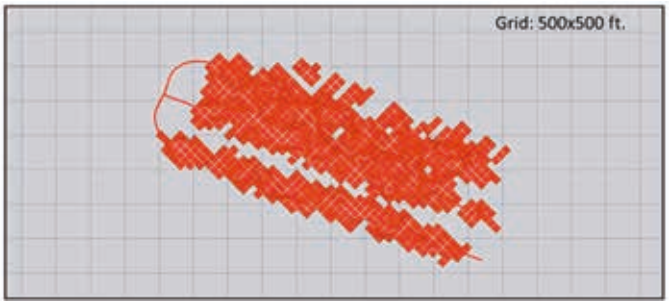

Figure 3. *Productive-SRV for all three wells illustrating rock volume between wells 1 and 3 that does not contain proppant filled fractures and is expected to be left undrained.*

and the J2 joints connect the longer, linear trends generated by the joints stimulated along the J1 direction. This information is invaluable as it tells the operator that both fracture sets are being activated.

A subset M-DFN is generated from the full M-DFN to evaluate proppant placement and estimate the productive part of the total stimulated rock volume. Estimating the propped half-length is performed by filling the subset M-DFN with proppant from the wellbore outward on a stage by stage basis. The packing density of the proppant is variable and can be adjusted based on the specific gravity of the proppant and fluid type. The northernmost well in Figure 2 has a propped half-length of 500 ft.

Evaluating proppant placement in the calibrated M-DFN allows operators to discern between the part of the stimulated rock volume (SRV) that contributes to production in the long-term from the part of the reservoir that was affected by the treatment, but may not be hydraulically connected over a longer period of time and only contributes to initial production. Figure 3 shows the total Productive-SRV™ for all three wells and captures the variation in the Productive-SRV volume realised for each well. The undrained reservoir between the centre and southernmost well suggests that wellbore spacing may be slightly reduced in order to provide a well-connected propped fracture network without any un-drained parts between wellbores.

Eagle Ford case study

In the Eagle Ford example the array used to acquire the data for the study wells can be seen in Figure 4. It consisted of 10 surface deployed arms and 1200 stations of seismic recording with six geophones per station. The total area under the array footprint is approximately 10 square miles. The high fold, wide azimuth and large aperture geometry of the monitoring array provides a consistent imaging resolution under the entire array and provides a high-confidence estimate of event magnitude. Another advantage compared to single well downhole monitoring is the capability to determine source mechanisms; a crucial input for the analysis presented in this case study.

The microseismic pointset acquired and processed during the 18 stage treatment of both wells can be seen in Figure 5 and shows that two types of source mechanisms occurred. While induced fracture related failure was recorded in a dip-slip mechanism indicating that the maximum principal stress is vertical, a pre-stressed, pre-existing feature was observed in the south southeast to north northwest direction failing in strike-slip mode. During the course of the treatment a large geohazard was activated and mapped from the toe of the wellbores extending approximately 4000 ft to the south southeast with a 160˚ strike. As seen in Figure 5, the events related to the geohazard reactivation were mostly strike-slip indicating a stress regime deviating from the in-situ stress conditions observed elsewhere in the area. The geohazard was continuously activated during the zipper-frac treatment from Stage 2 of well A through Stage 6 of well B, spanning around 2000 ft of lateral length. Most of the geohazard related events occurred during stages within a 500 ft radius of it. For maximum treatment efficiency on adjacent wellpads, the stimulation may be monitored over this 500 ft interval in real time in order to cease pumping when the feature is being activated.

An M-DFN workflow was applied to the microseismic pointset. Source mechanism analysis provided the strike and dip of the failure plane for individual events while the magnitude of the event along with rock rigidity and injected fluid volumes permitted estimating the length, height and aperture of the individual fractures. A proppant filling algorithm was then applied to the modelled fractures providing the proppant filled fracture network or Propped M-DFN as shown in Figure 6.

From the propped M-DFN in Figure 6 a conservative average propped half-length estimate of around 270 ft is observed for both wells

suggesting an ideal wellbore spacing of close to 540 ft. That means that the propped fractures from each well butt up against each other leaving very few unpropped fractures in between.

To properly understand the impact of the treatment schedule on fracture growth, one needs to look at the fracture growth as a function of time and injected slurry volumes. This is accomplished by analysing the fracture growth during the high viscosity proppant-laden gel phase of the treatment. The lateral distance of the microseismic events can be mapped with the injected fluid volume as seen in Figure 7. The blue curve is generated by running a moving average window through the microseismic data for all stages as a function of normalised average fluid volume. This identifies the average lateral distance of the fracture network front towards adjacent wells throughout the treatment. The graph shows how the low viscosity slickwater pad established the initial geometry of the fracture network while microseismicity concentrates closer to the wellbore after the introduction of high viscosity gel, indicating an increase in fracture width and near-wellbore complexity. Since the gel carries most if not all of the proppant, the microseismicity associated with the gel should give a good estimate of the proppant half-length. As seen in the plot, the average distance of the near-wellbore microseismicity is about 270 ft, which matches the half-length obtained from the proppant filled M-DFN.

Summary

Evaluating proppant placement in the calibrated DFN allows operators to separately indentify the part of the SRV that contributes to production in the long-term, and the part of the reservoir that was affected by the treatment but may not be hydraulically connected over a longer period of time and only contributes to initial production. As seen in the two examples presented, microseismic monitoring was used as a reservoir characterisation tool in order to further the understanding of hydraulic stimulation and evaluate the efficiency of a hydraulic fracturing treatment. With the use of source mechanisms, an M-DFN was modelled onto the microseismic events recorded during the treatment. With proppant placement analysis propped and unpropped parts of the M-DFN were identified implying productive and non-productive parts of the total SRV for long-term production. Deterministic analysis of the microseismic data presented here provides a unique methodology to quantify the realised fracture geometry and understand and optimise the treatment parameters on future wells.

References

1. Baig, A., and Urbancic, T., 'Microseismic moment tensors: A path to understanding frac growth', The Leading Edge, Vol. 29, pp. 320 - 324, (March, 2010).
2. Bohnhoff, M., Dresen, G., Ellsworth, W.L. and Ito, H., 'Passive Seismic Monitoring of Natural and Induced Earthquakes: Case Studies, Future Directions and Socio-Economic Relevance', New Frontiers in Integrated Solid Earth Sciences, International Year of Planet Earth, DOI 10.1007/978-90-481-2737-5_7, Springer, (2010).
3. Duncan, P.M. and Williams-Stroud, S., 'Marcellus Microseismic', Oil and Gas Investor, Vol. 10, pp. 65 - 67, (November, 2009).
4. McKenna, J.P., 'Verification of a Proppant-Filled Discrete Fracture Network Model', SPE 169496, SPE Western North American and Rocky Mountain Joint Regional Meeting, Denver, CO, USA, (April 16 - 18, 2014).
5. McKenna, J.P. and Toohey, N. 'A magnitude-based calibrated discrete fracture network methodology', First Break, v. 31:95-97, (2013).
6. Neuhaus, C.W., Telker, C., Ellison, M. and Blair, K., 'Hydrocarbon Production and Microseismic Monitoring – Treatment Optimization in the Marcellus Shale', SPE 164807, EAGE Annual Conference and Exhibition incorporating SPE Europec, London, UK, (June 10 - 13, 2013).
7. Nevarez, J.E. and Neale, C., 'Permanent Arrays Provide Critical Data', The American Oil & Gas Reporter, Vol. 52, (July, 2009).
8. Seibel M., Baig A. and Urbancic T., 'Single Versus Multiwell Microseismic Recording: What Effect Monitoring Configuration Has On Interpretation', SEG Technical Program Expanded Abstracts, pp. 2065 - 2069, (2010).
9. Williams-Stroud S., Eisner L., Hill A., Duncan P.M. and Thornton M.P., 'Beyond the Dots in the Box – Microseismicity-constrained Fracture Models for Reservoir Simulation', F018, EAGE Annual Conference and Exhibition incorporating SPE Europec, Barcelona, Spain, (June 14 - 17, 2010).
10. Williams-Stroud, S., Neuhaus, C.W., Telker, C., Remington, C., Barker, W.B., Neshyba, G. and Blair, K., 'Temporal Evolution of Stress States from Hydraulic Fracturing Source Mechanisms in the Marcellus Shale' SPE 162786, SPE Canadian Unconventional Resources Conference, Calgary, AB, Canada, (October 30 – November 1, 2012).

Figure 4. *Map view of microseismic surface array. Radial lines of altogether 7200 geophones can be seen in red. Wellbores A and B can be seen in blue.*

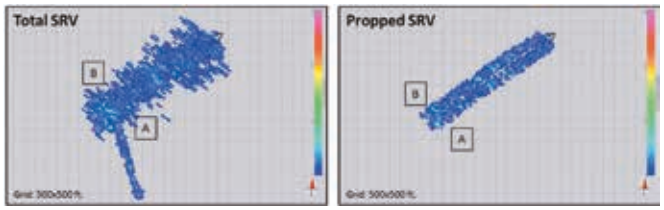

Figure 5. *Microseismic pointset for wells A and B. Events are coloured by their respective source mechanism and sized by magnitude.*

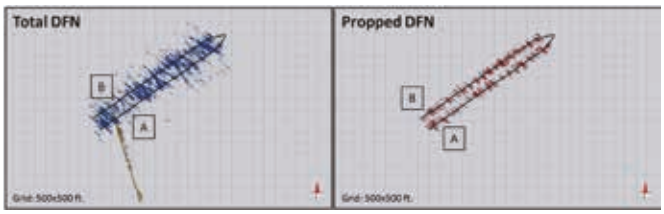

Figure 6. *M-DFN and proppant filled M-DFN for wells A and B.*

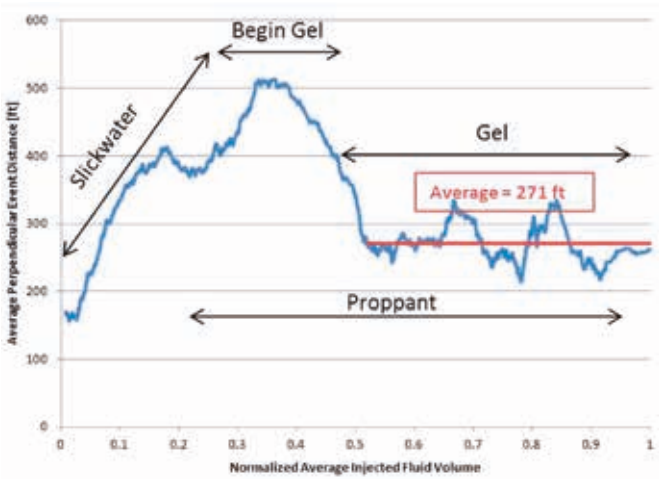

Figure 7. *Fracture network growth with injected fluid volume. The blue curve represents the average perpendicular event distance, obtained from a moving average window run through the microseismic data, in relation to the average injected fluid volume.*